Int. J. Heat Mass Transfer. Vol. 30, No. 10, pp. 2045–2057, 1987
Printed in Great Britain

0017–9310/87 $3.00 + 0.00

Prediction technique for minimum-heat-flux(MHF)-point condition of saturated pool boiling

SHIGEFUMI NISHIO

Institute of Industrial Science, University of Tokyo, 22-1, Roppongi, 7-chome, Minato-ku, Tokyo 106, Japan

(*Received* 30 *June* 1986)

Abstract—The temperature-controlled hypothesis for the minimum-heat-flux(MHF)-point condition, in which the MHF-point temperature is regarded as the controlling factor and is expected to be independent of surface configuration and dimensions, is inductively investigated for saturated pool boiling. In this paper such features of the MHF-point condition are experimentally proved first. Secondly, a correlation of the MHF-point temperature is developed for the effect of system pressure. Finally, a simple technique based on this correlation is presented to estimate the effects of surface configuration, dimensions and system pressure on the minimum heat flux.

1. INTRODUCTION

THE ASSESSMENT of the minimum condition to sustain film boiling continues to be an active branch of boiling-heat-transfer investigations. The need for such investigations is motivated under such circumstances as the reliability considerations of the ECCS in LWRs, the thermal stability analyses of superconductors, the advent of new materials produced by rapid quenching, and the modeling of vapor explosions. In the literature a number of terms have been used to describe the minimum point, e.g. minimum-heat-flux(MHF) point, minimum-film-boiling(MFB) point, quench point, rewetting point and Leidenfrost point. In any case, the minimum condition is described by its temperature T_M and heat flux q_M. In this paper, this minimum condition is termed 'the minimum-heat-flux(MHF)-point condition' (T_M, q_M).

1.1. *Background*

To investigate the controlling mechanism for the MHF point and to predict the MHF-point condition, some classical models have been proposed [1–6]. In each of these, however, one of the following hypotheses seems to be implicitly premised. The first is 'the temperature-controlled hypothesis', in which the MHF-point temperature T_M is regarded as the dominant factor that determines the MHF point and thus the value of T_M is analyzed. The other is 'the heat-flux-controlled hypothesis', in which the minimum heat flux q_M is regarded as the dominant one and the value of q_M is analyzed. Consequently, the typical models can be grouped into two major categories; 'the temperature-controlled model' and 'the heat-flux-controlled model'.

In the temperature-controlled models, the MHF-point temperature T_M is related to the so-called 'maximum wetting temperature' T_{lw} (i.e. $T_M = T_{lw}$). The typical model of this kind is the 'foam limit model' proposed by Spiegler *et al.* [1]. They proposed that 'the liquid's maximum, metastable superheat temperature' T_{ls} corresponds to the maximum wetting temperature (i.e. $T_M = T_{lw} = T_{ls}$). Segev and Bankoff [2] adopted the maximum temperature for adsorption T_{la} as the value of T_{lw} (i.e. $T_M = T_{lw} = T_{la}$). In the heat-flux-controlled models, on the other hand, the minimum heat flux q_M is related to a kind of critical energy density. The typical model of this kind is the hydrodynamic instability models proposed by Zuber [3], Berenson [4], Lienhard and Wong [5] and Lienhard and Dhir [6]. They supposed that the minimum heat flux q_M corresponds to the vapor production rate to sustain the natural rate of growth of unstable disturbances resulting from the Taylor instability at the vapor–liquid interface.

In addition to the above stated modeling approaches, there are a number of experimental studies of parametric effects on the MHF-point condition. The information obtained from such studies is summarized as follows [7].

(1) Effect of collapse mode of vapor film: Iloeje *et al.* [8] isolated three different controlling mechanisms for forced convection rewetting. These are, impulse-cooling collapse, axial-conduction-controlled collapse and dispersed-flow rewetting. The former two mechanisms are considered to exist also in pool boiling [7]. The conduction-controlled collapse means a collapse of vapor film associated with the precursory local collapse which propagates along the boiling surface at a rate controlled by thermal conduction in the surface. The impulse-cooling collapse means the spontaneous collapse of the vapor film without such a precursory collapse. Kovalev [9] and Nishio [10] reported the experimental evidence that the MHF-point condition for pool boiling is affected by the collapse mode of vapor film. Namely, the MHF-point condition upon impulse-cooling collapse is lower than that upon conduction-controlled collapse.

NOMENCLATURE

c_p	specific heat
D	diameter or representative length of boiling surface
F_c	instantaneous liquid–solid contact-area fraction
g	standard acceleration of gravity
Gr_D	Grashof number of vapor phase, $g(\rho_l-\rho_v)\rho_{vf}D^3/\mu_{vf}^2$
h_f	heat transfer coefficient of fully-developed film boiling
h_M	heat transfer coefficient at MHF point
Ja	modified Jacob number, $c_{pl}\Delta T_M/L$
k	thermal conductivity
l_c	one-dimensional critical wavelength, $2\pi\sqrt{(\sigma/g(\rho_l-\rho_v))}$
l_r	dimensionless characteristic length, $\sigma^3/g(\rho_l-\rho_v)^3\nu_l^4$
L	latent heat of vaporization
L_0	modified latent heat of vaporization
N_0	$L_0/(c_{pvf}\Delta T_{sat})$
Nu_D	Nusselt number
p	system pressure
p_{cr}	thermodynamic critical pressure
Pr_{vf}	Prandtl number of vapor phase
q_c	heat flux at liquid–solid contact area
q_d	heat flux at dry area
q_M	minimum heat flux
q_w	average wall heat flux
T_{cr}	thermodynamic critical temperature
T_{la}	maximum temperature for adsorption
T_{ls}	liquid's maximum, metastable superheat temperature
T_{lw}	maximum wetting temperature
T_M	MHF-point temperature
T_{sat}	saturation temperature
ΔT_M	surface superheat at MHF point
ΔT_{sat}	surface superheat
X	reduced temperature at saturation point, T_{sat}/T_{cr}
Y	dimensionless superheat at MHF point, $\Delta T_M(X)/[T_{cr}-T_{sat}(X)]$
Z	dimensionless superheat ratio, Y/Y^*.

Greek symbols

μ	absolute viscosity
ρ	density
ρ_r	density ratio, ρ_v/ρ_l
σ	surface tension
ν	kinematic viscosity.

Subscripts

co	prediction
ex	experiment
l	saturated liquid
v	saturated vapor
vf	vapor at film temperature
Mh	MHF point in high-pressure region
Mm	MHF point in intermediate-pressure region
Ml	MHF point in low-pressure region.

Superscripts

*	$X = 0.7$.

(2) Effect of surface configuration and dimensions: (2-1) Nishio [10] reported that experimental data of T_M for spherical surfaces are not dependent on the diameter. (2-2) Lienhard and Wong [5] showed that, for horizontal cylinders, the predictions on the effect of the diameter on the value of q_M from their hydrodynamic instability model were in qualitative agreement with their data.

(3) Effect of system pressure: (3-1) Sakurai *et al.* [11] found that the value of T_M upon impulse-cooling collapse approaches the liquid's maximum, metastable superheat temperature T_{ls} as system pressure increases. (3-2) However, data of T_M reported by Grigull and Abadzic [12], Sciance and Colver [13], Hesse [14], and Bier *et al.* [15] show that the value of T_M considerably exceeds even the critical temperature of the liquid at subcritical pressures. Furthermore, most of the data of T_M for various liquids at atmospheric pressure are much lower than the value of T_{ls} [7]. (3-3) Sciance and Colver [13], Nikolayev and Skripov [16], and Bier *et al.* [15] reported the experimental data that the value of q_M reaches a maximum at a reduced pressure p/p_{cr} of 0.2–0.4 and that the prediction from the hydrodynamic instability model has a good order-of-magnitude agreement with such a tendency. (3-4) However, Sakurai *et al.* [11] showed in their experiments of water that, at pressures from 0.1 to 2 MPa, the dependency of the impulse-cooling-collapse MHF on system pressure is much weaker than that predicted from the hydrodynamic instability model.

(4) Effect of liquid subcooling: (4-1) In most of the literature [17–21], it is reported that the value of T_M is linearly dependent on liquid subcooling. (4-2) Further, it is indicated that the value of T_M becomes much higher than the value of T_{ls} under large subcoolings. (4-3) However, Sakurai *et al.* [11] showed that the value of T_M upon impulse-cooling collapse becomes roughly equal to the value of T_{ls} under large subcoolings.

(5) Effect of liquid velocity: (5-1) Dhir and Purohit

[20] reported the experimental results indicating that the value of T_M for external flow is not dependent on liquid velocity in the range of 0–0.5 m s^{-1}. Groeneveld and Stewart [22] measured the value of T_M upon impulse-cooling collapse for inverted annular flow and developed a correlation indicating that the value of T_M is independent of mass velocity and quality. (5-2) However, Yilmaz and Westwater [23] reported the experimental results indicating that the value of T_M for external flow around a horizontal cylinder increases as the liquid velocity increases approximately beyond 4 m s^{-1}.

(6) Effect of surface conditions: Berenson [24], Bergles and Thompson [25], Veres and Florschuetz [26], Hasegawa *et al.* [27], Chowdhury and Winterton [28], and Bui and Dhir [29] showed that surface wettability including cleanliness has a strong effect on the MHF-point condition. In particular, Chowdhury and Winterton showed that the contact angle measured at the room temperature is a good index of the effects of surface wettability on transition-boiling heat transfer and also on the MHF-point condition.

(7) Effect of thermal conductance of boiling surface: Lin and Westwater [30], Berlin *et al.* [31] and Nishio [32, 33] showed that the MHF-point condition (T_M, q_M) increases with decreasing thermal conductance of the boiling surface.

(8) Effect of boiling process: Peyayopanakul and Westwater [34] and Nishio [33] showed that, for horizontal flat plates, the experimental data of T_M of quenching tests are not different, but data of q_M are lower, in comparison to the respective steady-state values. However, Veres and Florschuetz [26] and Sakurai *et al.* [35] reported that, for spherical and cylindrical surfaces, not only T_M but also q_M are independent of the boiling process (transient or steady state).

The above brief search of the literature reveals that there seems to be considerable uncertainty as to the parametric behavior of the MHF condition for a given liquid. As pointed out in ref. [7], nevertheless, it seems clear that both types of modeling do not give systematic predictions of the parametric behavior of the MHF-point condition in the entire range of parameters. Namely, the experimental findings stated in such items as (2-1), (3-1), (4-3), (5-1) and (8) appear to support the temperature-controlled hypothesis, but those in such items as (3-2), (4-2), (5-2), (6) and (7) indicate the incompletion of the classical models of this type. In contrast, the experimental findings in (2-2) and (3-3) seem to support the hydrodynamic instability model, but the models of this type do not predict precisely the pressure effects as stated in item (3-4). Furthermore, they do not account for the effects of surface orientation, liquid subcooling, liquid velocity, and surface conditions. Due to the above-stated unsatisfactoriness of both types of modeling, some advanced models and correlations have been proposed accounting for liquid–solid contact behavior by Baumeister and Simon [36], Henry [37], Nishio and Hirata [38] and Gunnerson and Cronenberg [39]. Neither of these approaches have been successful in systematic predictions of the MHF-point condition.

1.2. *Objectives*

From the above brief discussion it can be concluded that both the aforementioned hypotheses have not been substantiated. This appears to be one of the reasons why the controlling mechanism for the MHF point has not been made clear. In particular, the experimental findings stated in items (6) and (7) seem to be important because they indicate that the controlling mechanism for the MHF point is closely related to liquid–solid contact behavior. In general, the MHF-point condition appears to be the result of a delicate balance between film boiling heat transfer and the heat removal through intermittent local contacts. For example, the modeling approach for the post-CHF regimes uses the concept that at any instant, liquid makes contact with the heating surface over a certain part and vapor over the rest, leading to

$$q_w = F_c q_c + (1 - F_c) q_d \quad (1)$$

where F_c is the instantaneous liquid contact-area fraction, q_c the heat flux to the contacting liquid, and q_d is the heat flux to the vapor at the dry area [7]. Consequently, a better understanding of liquid–solid contact behavior is of importance in the modeling of the controlling mechanism at the MHF point. Unfortunately, available data of liquid–solid contact behavior such as F_c, q_c and q_d up to now have been quite limited [7].

Thus, in this paper, an inductive approach is chosen to clarify the MHF-point condition. Namely, an attempt to discuss the validity of the temperature-controlled hypothesis through the development of a correlation technique for the MHF-point condition has been made.

2. EFFECTS OF SURFACE CONFIGURATION AND DIMENSIONS

First, it will be discussed which hypothesis, of the temperature-controlled or heat-flux-controlled hypotheses, is adequate to develop a correlation. To do this, the effects of surface configuration and dimensions on the MHF-point condition are examined for saturated water and liquid nitrogen at atmospheric pressure using a horizontal, cylindrical surface of diameter D ranging from 0.3 to 9.6 mm.

2.1. *Experimental apparatus and data reduction*

Figure 1 shows the experimental apparatus. It includes a test section, a pressure chamber with a viewing window, a pressure line that is used to reduce the system pressure, and a flow line to start and maintain the boiling tests. The pressure line includes a vacuum pump and a mercury manometer, and the

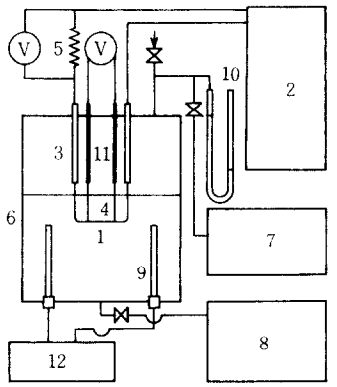

1.Platinum wire
2.DC Power supply
3.Electrode (I)
4.Platinum wire (0.05 mm)
5.Standard resistance
6.Vessel
7.Vacuum pump
8.Thermostat
9.Heater
10.Hg Manometer
11.Electrode (II)
12.AC Power supply

FIG. 1. Experimental apparatus.

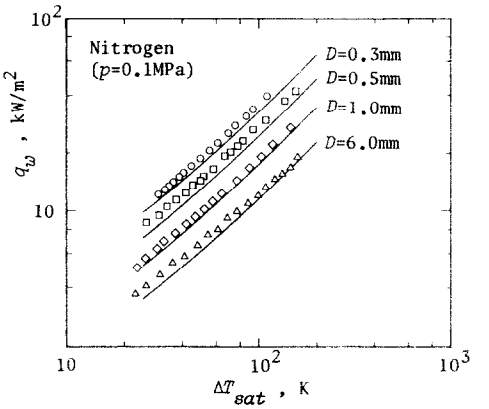

FIG. 2. Film-boiling curves of liquid nitrogen at atmospheric pressure (solid lines, Sakurai *et al.*'s correlation of fully-developed film-boiling heat transfer).

flow line includes a thermostatic vessel. These lines were used only for water experiments. The test section which is a horizontal, cylindrical surface was a platinum cylinder for $D = 0.3$–1.0 mm, and a copper tube of wall thickness of 1 mm for $D = 3.0$–9.6 mm. In order to avoid a precursory collapse of vapor film at the end of the heat transfer surface, all the cylindrical surfaces were made U-shaped and their ends were kept in the gas phase above the test liquid. In the case of a platinum cylinder, it was heated directly by a d.c. current supplied from a stabilized d.c. power supply and steady-state tests of film-boiling heat transfer were repeated by decreasing the d.c. current supply step by step down to the MHF-point condition. Two fine platinum wires 0.05 mm in diameter were spot welded to the platinum cylinder about 40 mm apart at the central portion of the cylinder, and were used as voltage taps. The voltage drop in the platinum cylinder was measured by these voltage taps, and the d.c. current was by measuring the voltage across a standard resistor inserted, in series, in the electric-current circuit. In these steady-state tests using platinum cylinders, surface temperatures were determined by the electrical resistance of the platinum cylinder and heat fluxes by Joule heating. It was found from a calibration test that the maximum error in temperature measurement was less than 0.5%. The steady-state tests were conducted for water and liquid nitrogen.

On the other hand, quenching tests of copper tubes from room temperature were conducted only for liquid nitrogen. In these quenching tests, surface temperatures were measured by Teflon-coated chromel–alumel thermocouples soldered at the surface from inside the tube, and heat fluxes were deduced from the temperature vs time data by using the lumped parameter approximation [40]. Here, it should be noted that Sakurai *et al.* [35] reported that the difference between the MHF-point conditions for quenching tests and steady-state tests is negligible for horizontal cylinders. The maximum uncertainty in heat flux due to the lumped parameter approximation occurred near the MHF point and it was estimated to be less than 1% because the Boit number at the MHF point is much less than 0.01.

An immersion heater located at the bottom of the chamber was used for water experiments to keep water at the saturation temperature. The heat transfer surface was wiped clean with acetone before all of the individual tests.

2.2. *Experimental results and discussions*

In Fig. 2, the film-boiling heat-transfer data of liquid nitrogen are shown for $D = 0.3$, 0.5, 1.0 and 6.0 mm. The solid lines in the figure are the predictions from the following correlation of the fully-developed, film-boiling, heat transfer coefficient h_f reported by Sakurai *et al.* [41]

$$Nu_D = K(Gr_D\, Pr_{vf}\, N_0)^{0.22}$$

$$K = 0.897 - 0.542 \log\left(\frac{l_c}{D}\right) + 0.439\left[\log\left(\frac{l_c}{D}\right)\right]^2 \quad (2)$$

where Nu_D, Gr_D, Pr_{vf}, N_0 and l_c denote the Nusselt number, the Grashof number of the vapor phase, the Prandtl number of the vapor phase, the ratio of the modified latent heat of vaporization to excess enthalpy of the vapor phase and the one-dimensional critical wavelength in the Taylor instability, respectively. The present film-boiling data show good agreement with the correlation, indicating that sufficient accuracy in temperature and heat-flux measurements has been realized in the present experiment.

In Fig. 3, the present data of the surface superheat at the MHF point ΔT_M for the horizontal cylinders are plotted against a representative length of boiling surface D for saturated water and liquid nitrogen at atmospheric pressure. For comparison, the existing data obtained for the horizontal flat plates, spheres and horizontal cylinders indicated by square, circular and triangular symbols, respectively, are plotted in

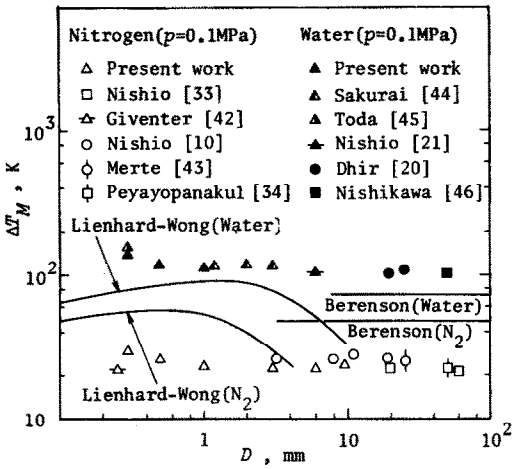

FIG. 3. Effects of surface configuration and dimensions on the surface superheat at the MHF point (triangular, circular and square symbols denote experimental data for horizontal cylinders, spheres and horizontal flat plates, respectively).

the figure. The representative length of the surface is regarded as the diameter for cylindrical, spherical and circular-flat-plate surfaces and the side length for square-flat-plate surfaces. The solid lines in the figure are the predictions from the hydrodynamic instability models proposed by Berenson (equation (3)) [4] and Lienhard and Wong [5]. Although Lienhard and Wong have not derived an analytical equation for the surface superheat at the MHF point, in this paper the values of ΔT_M for horizontal cylinders were derived from q_M/h_f by using equations (2) and (4)

$$\Delta T_M = 0.127\left(\frac{\rho_{vf}L_0 l_c}{2\pi k_{vf}}\right)\left[\frac{g(\rho_l-\rho_v)\mu_{vf}}{(\rho_l+\rho_v)^2}\right]^{1/3} \quad (3)$$

$$q_M = 0.096\left(\frac{\rho_{vf}L_0 l_c}{\pi D}\right)\left[\frac{g\sigma(\rho_l-\rho_v)}{(\rho_l+\rho_v)^2}\right]^{1/4} \times\left[2+\left(\frac{l_c}{\pi D}\right)^2\right]^{-1/4}. \quad (4)$$

Figure 3 shows the following important features of the MHF-point temperature (or superheat). The first is the fact that the data of the MHF-point temperature for horizontal cylinders are almost independent of the diameter. The second is that the above result is also confirmed by the plots for spherical surfaces, and the third is that the numerical value of the MHF-point temperature obtained for horizontal cylinders is in good agreement with those for other surface configurations. Consequently, from Fig. 3, it can be concluded that the MHF-point temperature (or superheat) is not sensitive to surface configuration and dimensions, while, as shown later, the minimum heat flux is, of course, dependent on them.

Now, in the discussion to follow, attention will be focused on the MHF-point condition under the following fixed situation.

(a) Saturated pool boiling under the standard gravitational acceleration.

(b) Smooth and clean surfaces made of a good thermal conductor.

(c) Effect of conduction-controlled collapse associated with a precursory-local collapse is weak.

As it has been stated in the introduction, the possible parameters on the MHF-point condition are considered to be the following in general; collapse mode, surface configuration and dimensions, system pressure, liquid subcooling and velocity, gravitational acceleration, surface wettability, thermal conductance of surface, and boiling process (i.e. transients or steady states). Thus, under the fixed conditions such as items (a)–(c), surface configuration and dimensions, system pressure, surface wettability, and boiling process remain as the possible parameters on the MHF-point condition. On the other hand, the experimental results stated above indicate that the MHF-point temperature is independent of surface configuration and dimensions. Further, as it has been stated in the introduction, there are several experiments showing that the MHF-point temperature during quenching tests is not different from that in steady-state tests. Consequently, the MHF-point temperature for a given liquid under the fixed conditions such as items (a)–(c) is to be considered as a function only of system pressure and surface wettability.

Here, it should be noted that, in the modeling approach based on the temperature-controlled hypothesis, it is the usual/physical way to premise that the MHF-point temperature upon impulse-cooling collapse for saturated boiling on a good thermal conductor is a function only of physical properties of boiling fluid and surface wettability [36]. This feature of the temperature-controlled hypothesis is consistent in the above-stated feature of the MHF-point temperature. This is one of a few reasons that, in this paper, the temperature-dominant approach is considered to be superior to the heat-flux-dominant approach.

3. CORRELATION OF MHF-POINT TEMPERATURE

In this section, the validity of the temperature-controlled hypothesis will be discussed through the development of a correlation technique for the MHF-point temperature. From the discussion in the previous section, the MHF-point temperature under the fixed conditions such as items (a)–(c) is expected to be a function only of system pressure and surface wettability. Although some correlations for the MHF-point temperature [36, 47] account for the degree of surface wettability, the surface wettability on a high temperature surface has not been quantified [37], and thus, in this paper, it is supposed for simplicity that the surface wettability for a given, ordinary liquid is almost the same on common, clean metal surfaces for

Table 1. Data sources

Liquid	p/p_{cr}	Geometry	Ref.
Water	0.0046–0.89	Wire (2, 3 mm)	[44]
Propane	0.05–0.72	Cylinder (20.6 mm)	[13]
n-Hexane	0.033–0.91	Cylinder (3.3 mm)	[48]
Ethanol	0.0055–0.11	Plate (—)	[49]
R-113	0.012–0.23	Plate (62 mm)	[50]
R-114	0.092–0.61	Cylinder (14 mm)	[14]
RC-318	0.16–0.98	Cylinder (8 mm)	[15]
Nitrogen	0.030–0.15	Sphere (25.4 mm)	[51]

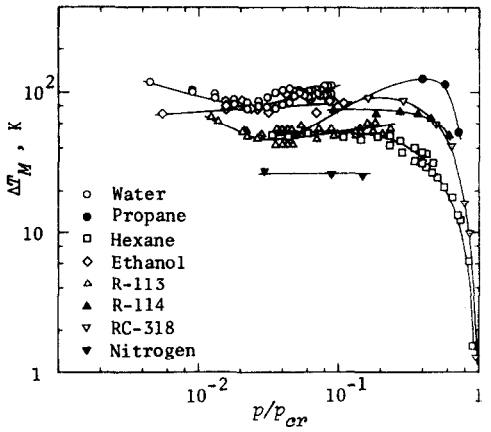

FIG. 4. Effect of pressure on the surface superheat at the MHF point.

engineering use. On this assumption, the MHF-point temperature for a given, ordinary liquid on a common, clean metal surface is expected to be a function only of system pressure. However, this assumption is only first order at best and the result must be evaluated in this light.

3.1. *General aspects of the* $\Delta T_M - p$ *relation*

The existing sources of data of the pressure effect on the MHF-point temperature for saturated pool boiling are tabulated in Table 1, and these data are shown in Fig. 4 as a plot of the surface superheat at the MHF point ΔT_M vs the reduced pressure p/p_{cr}. From Fig. 4, the following features can be pointed out of the relation between ΔT_M and system pressure.

(1) For low pressures, the slope of the ΔT_M vs p/p_{cr} plot is negative.

(2) For intermediate pressures, the slope is slightly positive or nearly equal to 0.

(3) For high pressures, the slope is again negative.

In this paper, these pressure regions categorized by the slope of the ΔT_M–p relation are termed from now onwards 'the low-pressure region', 'the intermediate-pressure region', and 'the high-pressure region' in the order of increasing pressure.

Since the available data on the ΔT_M–p relation are limited as shown in Table 1, it should be noted that such a classification should be checked again in future

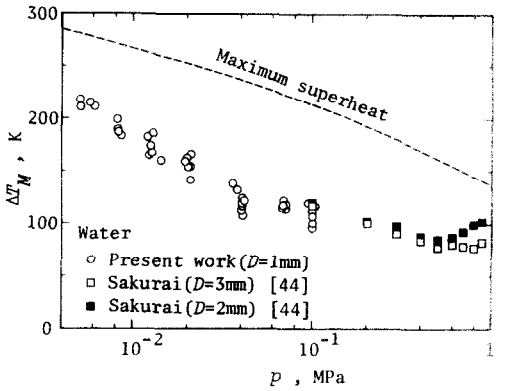

FIG. 5. Effect of pressure on the surface superheat at the MHF point of water in the low-pressure region.

experiments. In particular, data in the low-pressure region are quite limited, and thus, in this section, the existence of the low-pressure region will be confirmed for saturated water. From Fig. 4, the low-pressure region for water is expected to appear at pressures approximately lower than 0.4 MPa. Thus, experiments for pool film boiling were conducted for saturated water at subatmospheric pressures using the experimental apparatus shown in Fig. 1. In this experiment, a U-shaped platinum cylinder 1 mm in diameter was used as the boiling surface. The experimental procedure and data reduction are the same as those mentioned in Section 2.1.

The present data on the ΔT_M–p relation at subatmospheric pressures are plotted in Fig. 5 along with the experimental data of Sakurai *et al.* [44]. This figure shows that good agreement is obtained between the present and Sakurai *et al.*'s data and also that the low-pressure region, in which the value of ΔT_M decreases as system pressure increases with the value of T_M smaller than the liquid's maximum, metastable superheat temperature (dashed line in Fig. 5), does exist.

3.2. *Screening of data sources*

Some groups of data plotted in Fig. 4 are located at temperatures much higher than the thermodynamic critical temperature of the liquid T_{cr}. At present, however, it seems to be the general consensus that intimate liquid–solid contacts may not occur at surface temperatures beyond the liquid's maximum, metastable superheat temperature [49]. Further, as it has been stated in the introduction, there are some data suggesting that the MHF-point temperature upon impulse-cooling collapse does not exceed the liquid's maximum, metastable superheat temperature even under high-pressure/large-subcooling conditions. Thus, it is considered that the experiments in which the value of T_M is higher than the thermodynamic critical temperature were not conducted under the impulse-cooling collapse of vapor film but under the conduction-controlled collapse. For this reason, in this paper, only those sources of data in which any

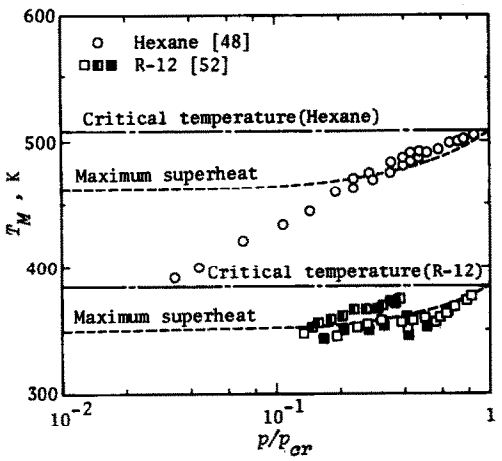

FIG. 6. Comparison between the liquid's maximum, metastable superheat temperature (maximum superheat) and the MHF-point temperature in the high-pressure region.

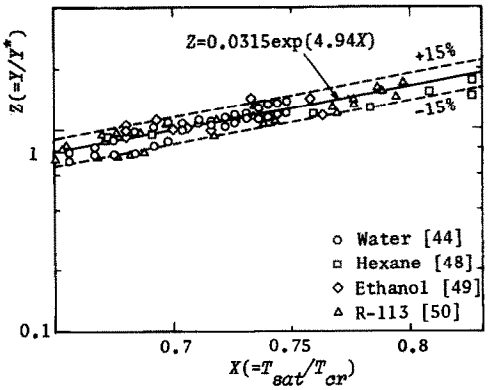

FIG. 7. Effect of pressure on the surface superheat at the MHF point in the intermediate-pressure region.

data of T_M not exceeding the thermodynamic critical temperature have been selected.

3.3. *Correlation of MHF-point temperature in high-pressure region*

The above-stated screening of the data sources in the literature reveals that the following data are available to develop a correlation in the high-pressure region. They are, the data for n-hexane on a horizontal cylinder [48] and Freon R-12 on a downward-facing conical surface [52]. In Fig. 6, these data are plotted vs the reduced pressure p/p_{cr}. The dashed lines in the figure are the predictions of the liquid's maximum, metastable superheat temperature T_{ls} from the correlation developed by Lienhard [53]. At high pressures, both sets of data plotted in the figure fall close to the respective dashed line. Thus, in this paper, the pressure region where the MHF point is controlled by the liquid's maximum, metastable superheat temperature is defined as 'the high-pressure region'. Consequently, using Lienhard's correlation for the liquid's maximum, metastable superheat temperature T_{ls}, the correlation for the MHF-point temperature in the high-pressure region is

$$T_M = T_{Mh} = T_{ls} = (0.905 - X + 0.095X^8)T_{cr} + T_{sat} \tag{5}$$

where X denotes the reduced temperature at the saturation point.

3.4. *Correlation of MHF-point temperature in intermediate-pressure region*

The intermediate-pressure region is defined as the region where the slope of the ΔT_M–p relation is slightly positive (or nearly equal to 0) with the value of T_M lower than T_{ls}. After the aforementioned screening of the data sources tabulated in Table 1, a survey of the available data sources focusing attention on the intermediate-pressure region, reveals that, for every liquid, the system pressure corresponding to the reduced saturation temperature $X(=T_{sat}/T_{cr}) = 0.7$ is included in this pressure region. Thus, the data which belong to the intermediate-pressure region are picked up from the available data source, and they are plotted in Fig. 7 as a plot of the dimensionless superheat ratio at the MHF point $Z = Y/Y^*$ vs X, where Y denotes $\Delta T_M(X)/[T_{cr} - T_{sat}(X)]$ and Y^* the value of Y at $X = 0.7$. As shown in Fig. 7, such a non-dimensional plot provides a similar relation for the four liquids. The solid line in the figure is the best fit curve for the data. This equation is

$$Z = 0.0315 \exp(4.94X) \tag{6}$$

or

$$T_M = 0.0315\Delta T_M^* \left(\frac{T_{cr} - T_{sat}}{T_{cr} - T_{sat}^*}\right) \exp(4.94X) + T_{sat}. \tag{7}$$

At this point, it remains to develop a correlation of the numerical value of ΔT_M^* (i.e. ΔT_M at $X = 0.7$). The numerical values of ΔT_M^* for various liquids are tabulated in the right-hand column of Table 2. These values are determined through the following procedure. In the cases of the liquids for which experimental data of ΔT_M^* have been reported, the experimental values are directly adopted if it can be confirmed that experimental data of ΔT_M in the report at other pressures agree with those for other surface geometries (this check is shown in the third column of Table 2). The numerical values determined through this procedure are marked with arrows in the right-hand column of Table 2. As for the liquids for which data of ΔT_M^* are not available, the numerical value of ΔT_M^* is determined by extrapolating an experimental value of ΔT_M at atmospheric pressure using equation (7). Also in this case, the accuracy of the base value of ΔT_M used is checked by comparison with data for other surface geometries (the third column of Table 2). The numerical values determined through this procedure are marked with circles in the right-hand column of Table 2.

Here, although the controlling mechanism of the MHF point in the intermediate-pressure region has not been made clear, it is supposed that the non-

Table 2. Numerical values of the surface superheat of the MHF point at $X = 0.7$

Liquid	Geometry	$\Delta T_M(X)$	Ref.	ΔT_M^*
Water	Plate	110(0.576)	[46]	
	Wire	117(0.576)	[44]	→ 96.4
	Cylinder	104(0.576)	[21]	
	Sphere	101(0.576)	[20]	
n-Pentane	Plate	59(0.659)	[24]	○ 62
	Plate	58(0.659)	[54]	
n-Hexane	Cylinder	41(0.845)	[48]	→ 49.4
	Plate	38(0.850)	[54]	
Ethanol	Plate	80(0.681)	[49]	→ 77.0
	Cylinder	72(0.681)	[55]	
CCl_4	Plate	79(0.628)	[24]	○ 90
	Plate	85(0.628)	[56]	
R-12	Plate	49(0.623)	[10]	○ 59
	Sphere	55(0.623)	[10]	
R-22	Plate	58(0.629)	[10]	○ 62
	Sphere	56(0.629)	[10]	
R-113	Plate	51(0.658)	[50]	→ 53.0
	Sphere	55(0.658)	[26]	
Nitrogen	Plate	22(0.613)	[34]	
	Plate	22(0.613)	[33]	
	Sphere	25(0.613)	[51]	→ 24.1
	Sphere	26(0.613)	[10]	

wetting condition in this pressure region is controlled by a balance between the movement of the wetting front and the boiling nucleation at the wetting front. Supposing such a mechanism, the following properties can be considered to be related to the surface superheat at the MHF point in the intermediate-pressure region; namely, liquid and vapor densities, dynamic viscosity, specific heat and thermal diffusivity of liquid, latent heat of vaporization, surface tension, and gravitational acceleration. From a dimensional analysis of these properties, the dimensionless dominant variables in the intermediate-pressure region become the following; the modified Jakob number $Ja(=c_{pl}\Delta T_M/L)$, the density ratio $\rho_r(=\rho_v/\rho_l)$, the Prandtl number of liquid Pr_l and the dimensionless characteristic length $l_r(=\sigma^3/g(\rho_l-\rho_v)^3\nu_l^4)$. The numerical values of ΔT_M^* listed in the right-hand column of Table 2 are correlated by a least squares approximation to these dimensionless variables by

$$Ja^* = 0.01095(\rho_r^*)^{0.6302}(Pr_l^*)^{1.008}(l_r^*)^{0.2056}. \quad (8)$$

In this equation, the asterisked dimensionless variables are those evaluated by the properties at $X = 0.7$. In Fig. 8, the experimental values listed in the right-hand column of Table 2 $(\Delta T_M^*)_{ex}$ are compared with the predictions from equation (8) $(\Delta T_M^*)_{co}$.

Finally, combining equations (7) and (8), the following equation is obtained as the correlation in the intermediate-pressure region.

$$T_M = T_{Mm} = 3.449\times10^{-4}\left(\frac{T_{cr}-T_{sat}}{T_{cr}-T_{sat}^*}\right)\left(\frac{L^*}{c_{pl}^*}\right)$$
$$\times(\rho_r^*)^{0.6302}(Pr_l^*)^{1.008}(l_r^*)^{0.2056}\exp(4.94X)+T_{sat}. \quad (9)$$

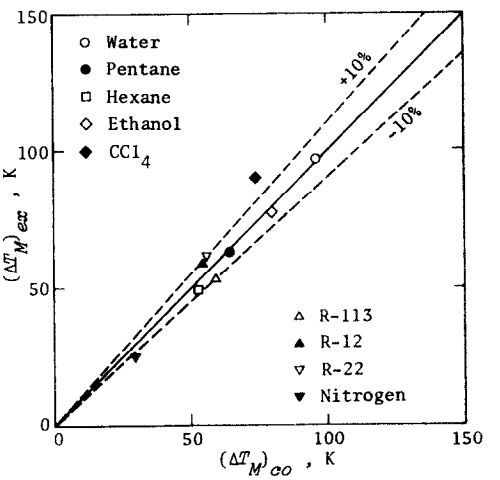

FIG. 8. Accuracy of the present correlation of ΔT_M at $X = 0.7$.

3.5. *Correlation of MHF-point temperature in low-pressure region*

As it has been stated, data in the low-pressure region are quite limited. Thus, in this paper, only a correlation for water is developed. From Fig. 4, the boundary between the intermediate- and low-pressure regions for water is estimated to be about $p/p_{cr} = 0.02$ and this value corresponds to $X = 0.65$. Deriving a correlating equation in the low-pressure region for water to meet the value of equation (9) at $X = 0.65$, the following correlation is obtained:

$$T_M = T_{Ml} = (T_{sat}+87.6)+5556(0.65-X)^{2.23}. \quad (10)$$

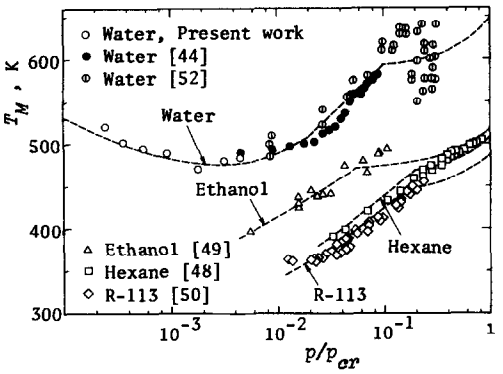

FIG. 9. Effect of pressure on the MHF-point temperature (dashed lines, present correlation).

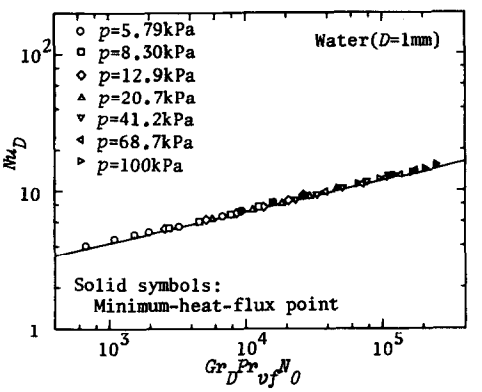

FIG. 10. Heat transfer coefficients at the MHF point (solid line, Sakurai *et al.*'s correlation of fully-developed film-boiling heat transfer).

3.6. *Comparison between experimental data and present correlations*

In Fig. 9, the predictions from the present correlations (i.e. equations (5), (9) and (10)) are compared with all the experimental data selected through the aforementioned screening. It is considered that they are in reasonable agreement with the data. This success in developing a correlation technique based on the temperature-controlled approach is the second reason that the validity of the temperature-controlled hypothesis is emphasized in this paper. Further, the data of Hein *et al.* [52] plotted in Fig. 9 were obtained for a downward-facing conical surface. Focusing attention on the Taylor instability at the vapor–liquid interface, vapor film around the surface of this type is considered stable. Though the data of Sakurai *et al.* [44] plotted in Fig. 9 are for a horizontal cylinder, these data are not remarkably different from those of a downward-facing conical surface contrary to the fact that the vapor film around a horizontal cylinder is disturbed by the Taylor instability. This result also supports the fact, as mentioned in Section 2.2, that the temperature-controlled hypothesis is superior to the heat-flux-controlled hypothesis.

4. ESTIMATION OF MINIMUM HEAT FLUX

In this section, the other condition at the MHF point, the minimum heat flux q_M, will be estimated from the viewpoint of the temperature-controlled approach. To do this, it is necessary to know the heat transfer coefficient h_M at the MHF point. So long as this value h_M is known, the minimum heat flux can be estimated by coupling the present correlations of the MHF-point temperature with the following conventional equation:

$$q_M = h_M \times \Delta T_M. \tag{11}$$

It is well known that there are a number of correlations for h_f (the heat transfer coefficient in fully-developed film boiling under saturated pool conditions). Nishio [10] and Bier *et al.* [15] reported that, even at the MHF point, the film boiling curve agrees with the prediction from a correlation for fully-developed film boiling. In order to check this, the present data of film-boiling heat transfer obtained in the experiments in Section 3.1 are compared in Fig. 10 with the correlation for fully-developed film boiling around horizontal cylinders presented by Sakurai *et al.* (equation (2)) [41]. The solid symbols in the figure indicate the data at the MHF point. The film boiling data are in good agreement with Sakurai *et al.*'s correlation (solid line) even at the MHF point. Thus, in this paper, the heat transfer coefficient at the MHF point h_M upon impulse-cooling collapse is estimated by $h_f(\Delta T_M)$ using the conventional correlations for fully-developed film boiling. Consequently, equation (11) can be rewritten as

$$q_M = h_M \times \Delta T_M = h_f(\Delta T_M) \times \Delta T_M. \tag{12}$$

As for the film-boiling heat-transfer correlations, the following proven correlations were used. They are, Sakurai *et al.*'s correlation for a horizontal cylinder (equation (2)), Grigoriev *et al.*'s for a spherical surface [57], and the correlations for a horizontal flat-plate surface developed by Klimenko [58] and Sauer and Ragsdell [59].

In Fig. 11, most of the existing data of the minimum heat flux for liquids at atmospheric pressure are compared with the predictions from the present technique (solid and dashed lines). In the figures, the predictions from the hydrodynamic instability models [4, 5] are also plotted (dotted lines). As it can be seen from them, the present simple technique to estimate the minimum heat flux can describe the effects of surface configuration and dimensions on the minimum heat flux. In Fig. 12, such a comparison is made for the effect of system pressure with the data of water for horizontal cylindrical surfaces and with those of Freon and nitrogen for a horizontal flat plate and spherical surfaces, respectively [50, 51]. Once again good agreement between the present technique and the experimental data is observed while the hydrodynamic instability models (dotted lines) predict a much stronger effect of system pressure on the mini-

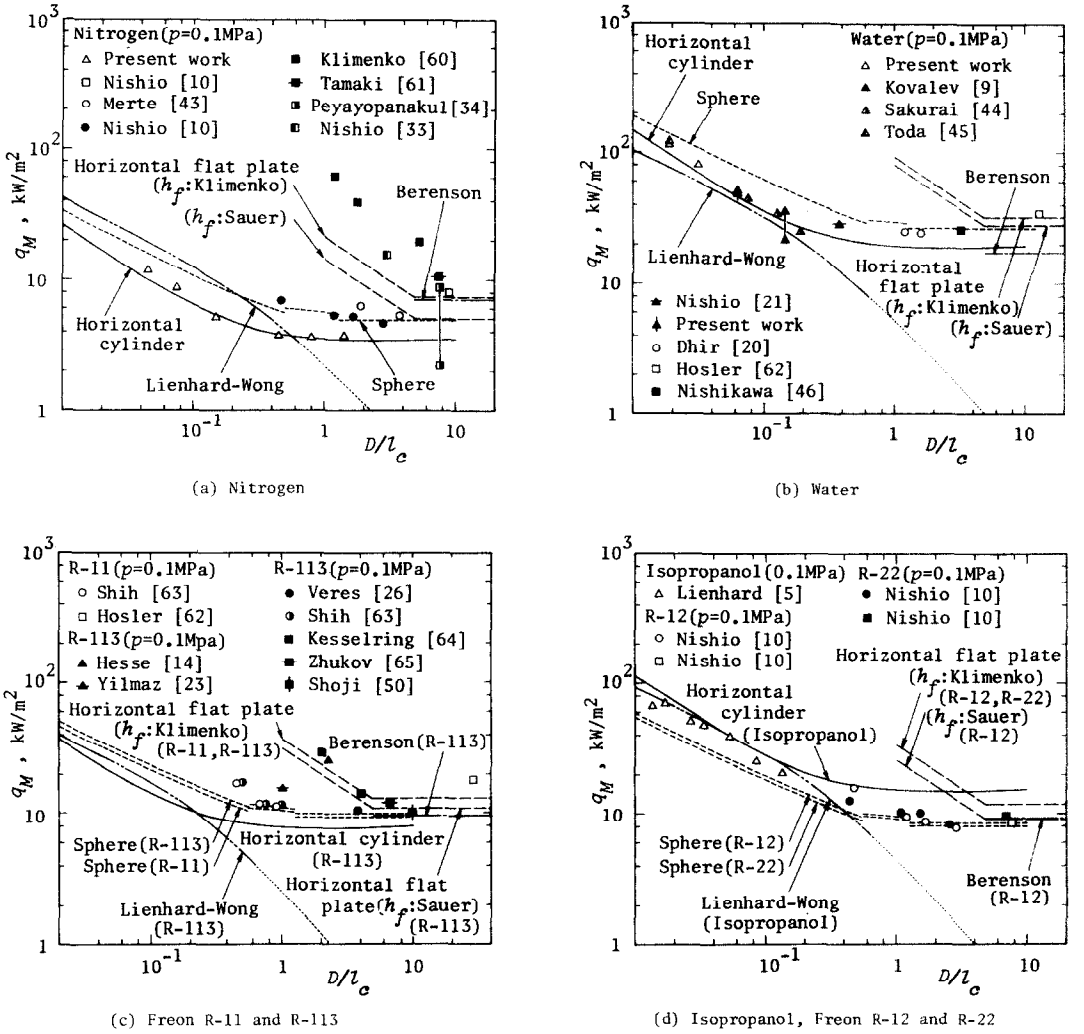

FIG. 11. Effects of surface configuration and dimensions on the minimum heat flux at atmospheric pressure (triangular, circular and square symbols denote experimental data for horizontal cylinders, spheres and horizontal flat plates, and solid and dashed lines denote the present predictions for horizontal cylinders, horizontal flat plates and spheres, respectively): (a) nitrogen; (b) water; (c) Freon R-11 and R-113; (d) isopropanol, Freon R-12 and R-22.

mum heat flux. These successes of the present technique in the prediction of the minimum heat flux are the third reason that the validity of the temperature-controlled hypothesis is emphasized in this paper.

In Fig. 13, the predictions from the present technique (solid lines) are compared with the data for horizontal cylinders reported by Grigull and Abadzic [12] and Nikolayev and Skripov [16]. In contrast to Figs. 11 and 12, there are considerable discrepancies between these data and the predictions even at atmospheric pressure. Similar results are observed in comparison with the data for horizontal cylinders of Hesse [14] and Bier *et al.* [15]. A possible reason for such discrepancies may be due to the effect of the precursory collapse of vapor film at the ends of cylindrical surfaces. As pointed out by Kovalev [9] and Hesse *et al.* [66], a precursory collapse of the vapor film at the ends of the horizontal cylinders permits the occurrence of nucleate boiling coexisting with film boiling at the central part and leads to a higher value of the minimum heat flux.

5. CONCLUSIONS

The temperature-controlled hypothesis for the MHF-point condition was inductively investigated through the development of a correlation technique for the MHF-point condition. Though the discussion presented here is limited to the MHF-point condition upon impulse-cooling collapse for saturated pool boiling under the standard gravitational acceleration on a clean and smooth surface made of a good thermal conducter, the following conclusions can be drawn.

(1) The MHF-point temperature under the above stated conditions is not dependent on surface con-

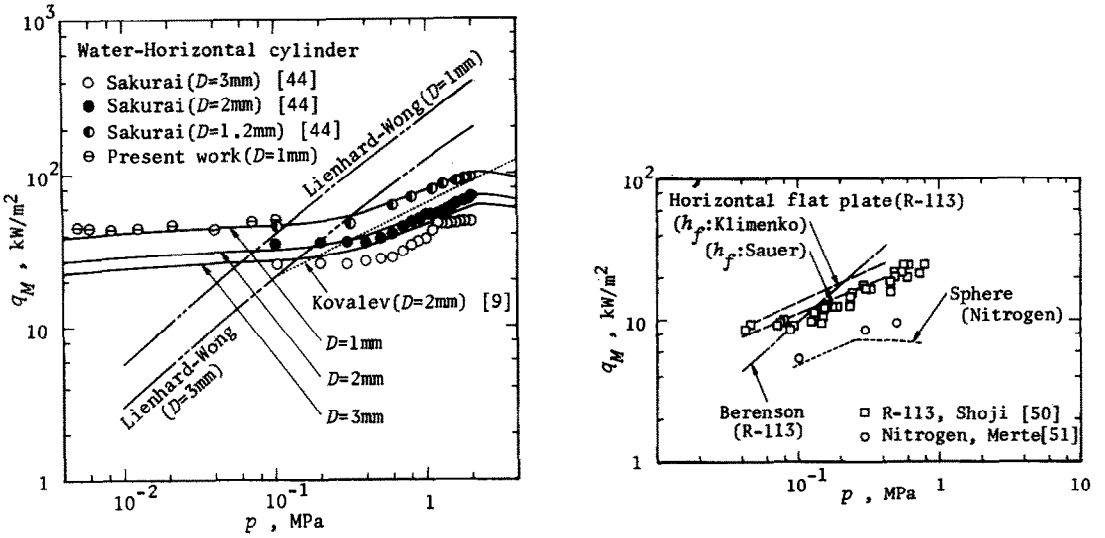

FIG. 12. Effect of pressure on the minimum heat flux (solid and dashed lines, present predictions): (a) water; (b) nitrogen and Freon R-113.

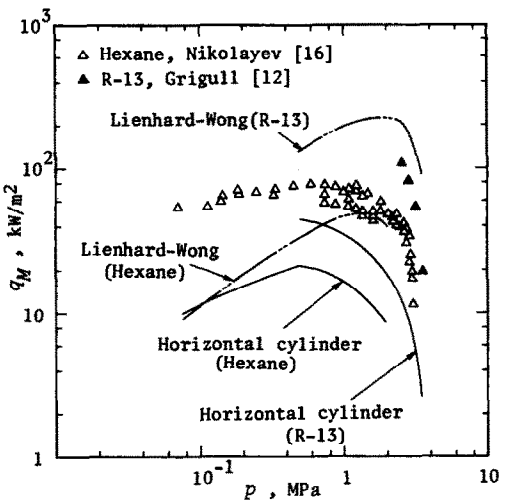

FIG. 13. Effect of pressure on the minimum heat flux upon conduction-controlled collapse (solid lines, present predictions).

figuration and dimensions. The temperature-controlled hypothesis for the MHF-point condition is consistent in this feature.

(2) A correlation technique for the MHF-point temperature was developed by dividing the pressure region into the following three regions: the low-, the intermediate- and the high-pressure regions. The correlations developed here agree well with experimental data as for the effects of system pressure.

(3) A simple estimation technique for the minimum heat flux was developed by coupling the present correlation for the MHF-point temperature with the conventional film boiling correlation. Relatively good agreement between the predictions and the data as for the effects of surface configuration, dimensions and system pressure were observed.

(4) All the above-stated results support the validity of the temperature-controlled hypothesis for the MHF-point condition.

REFERENCES

1. P. Spiegler, J. Hopenfeld, M. Silberberg, C. F. Bumpus, Jr. and A. Norman, Onset of stable film boiling and the foam limit, *Int. J. Heat Mass Transfer* **6**, 987–994 (1963).
2. A. Segev and S. G. Bankoff, The role of adsorption in determining the minimum film boiling temperature, *Int. J. Heat Mass Transfer* **23**, 637–642 (1980).
3. N. Zuber, Hydrodynamic aspects of boiling heat transfer, USAEC Report No. AECU-4439, University of California, Los Angeles (1959).
4. P. J. Berenson, Film boiling heat transfer from a horizontal surface, *Trans. Am. Soc. Mech. Engrs*, Series C, *J. Heat Transfer* **83**, 351–362 (1961).
5. J. H. Lienhard and P. T. Y. Wong, The dominant unstable wavelength and minimum heat flux during film boiling on a horizontal cylinder, *Trans. Am. Soc. Mech. Engrs*, Series C, *J. Heat Transfer* **86**, 220–226 (1964).
6. J. H. Lienhard and V. K. Dhir, On the prediction of the minimum pool boiling heat flux, *Trans. Am. Soc. Mech. Engrs*, Series C, *J. Heat Transfer* **102**, 457–460 (1980).
7. S. Nishio, Minimum heat flux condition in boiling heat transfer, NUREG/CP-0060, *Proc. First International Workshop on Fundamental Aspects of Post-dryout Heat Transfer*, pp. 137–169. U.S. Nucl. Reg. Com., Washington (1984).
8. O. C. Iloeje, D. N. Plummer, W. M. Rohsenow and P. Griffith, An investigation of collapse and surface rewet in film boiling in forced vertical flow, *Trans. Am. Soc. Mech. Engrs*, Series C, *J. Heat Transfer* **97**, 166–172 (1975).
9. S. A. Kovalev, An investigation of minimum heat fluxes in pool boiling of water, *Int. J. Heat Mass Transfer* **9**, 1219–1226 (1966).
10. S. Nishio, Study of minimum heat flux point of boiling heat transfer around a sphere, *Trans. Jap. Soc. Mech. Engrs*, Series B **49**, 1185–1194 (1983).
11. A. Sakurai, M. Shiotsu and K. Hata, Steady and unsteady film boiling heat transfer at subatmospheric

and elevated pressures, *Proc. ICHMT Seminar, Nuclear Reactor Safety Heat Transfer*, pp. 301–307. Hemisphere, Washington (1981).
12. U. Grigull and E. Abadzic, Heat transfer from a wire in the critical region, *Proc. Instn Mech. Engrs* **182** (3I), 52–57 (1967–68).
13. C. T. Sciance and C. P. Colver, Minimum film-boiling point for several light hydrocarbons, *Trans. Am. Soc. Mech. Engrs*, Series C, *J. Heat Transfer* **92,** 659–661 (1970).
14. G. Hesse, Heat transfer in nuclete boiling, maximum heat flux and transition boiling, *Int. J. Heat Mass Transfer* **16,** 1011–1027 (1973).
15. K. Bier, H. R. Engelhorn and D. Gorenflo, Heat transfer at burnout and Leidenfrost point for pressures up to critical. In *Heat Transfer in Boiling* (Edited by E. Hahne and U. Grigull), pp. 77–97. Hemisphere, Washington (1977).
16. G. P. Nikolayev and V. P. Skripov, Experimental investigation of minimum heat fluxes at submerged surfaces in boiling, *Heat Transfer—Sov. Res.* **2,** 122–127 (1970).
17. W. S. Bradfield, On the effect of subcooling on wall superheat in pool boiling, *Trans. Am. Soc. Mech. Engrs*, Series C, *J. Heat Transfer* **89,** 269–270 (1967).
18. M. M. K. Farahat, D. T. Eggen and D. R. Armstrong, Pool boiling in subcooled sodium at atmospheric pressure, *Nucl. Sci. Engng* **53,** 240–253 (1974).
19. M. M. K. Farahat, D. R. Armstrong and D. T. Eggen, Transient heat transfer between hot metal spheres and subcooled water, *Atomkernenergie* **29,** 17–22 (1977).
20. V. K. Dhir and G. P. Purohit, Subcooled film-boiling heat transfer from spheres, *Nucl. Engng Des.* **47,** 49–66 (1978).
21. S. Nishio and M. Uemura, Experimental study on cooling power of pool water, *J. Jap. Soc. Heat Treatment* **23,** 260–265 (1983).
22. D. C. Groeneveld and J. C. Stewart, The minimum film boiling temperature for water during film boiling collapse, *Proc. 7th Int. Heat Transfer Conf.*, Vol. 4, pp. 393–398 (1982).
23. S. Yilmaz and J. W. Westwater, Effect of velocity on heat transfer to boiling Freon-113, *Trans. Am. Soc. Mech. Engrs*, Series C, *J. Heat Transfer* **102,** 26–31 (1980).
24. P. J. Berenson, Experiments on pool-boiling heat transfer, *Int. J. Heat Mass Transfer* **5,** 985–999 (1962).
25. A. E. Bergles and W. G. Thompson, Jr., The relationship of quench data to steady-state pool boiling data, *Int. J. Heat Mass Transfer* **13,** 55–68 (1970).
26. D. R. Veres and L. W. Florschuetz, A comparison of transient and steady-state pool-boiling data obtained using the same heating surface, *Trans. Am. Soc. Mech. Engrs*, Series C, *J. Heat Transfer* **93,** 229–231 (1971).
27. S. Hasegawa, R. Echigo and K. Koga, Maximum heat fluxes for pool boiling on partly poor wettable heating surfaces (Part 1, on the visual observation of boiling and the temperature profiles of heating surface), *Bull. Jap. Soc. Mech. Engrs* **20,** 873–882 (1969).
28. S. K. R. Chowdhury and R. H. S. Winterton, Surface effects in pool boiling, *Int. J. Heat Mass Transfer* **28,** 1881–1889 (1985).
29. T. D. Bui and V. K. Dhir, Transition boiling heat transfer on a vertical surface, *Trans. Am. Soc. Mech. Engrs*, Series C, *J. Heat Transfer* **107,** 756–763 (1985).
30. D. Y. T. Lin and J. W. Westwater, Effect of metal thermal properties on boiling curves obtained by the quenching method, *Proc. 7th Int. Heat Transfer Conf.*, Vol. 4, pp. 155–160 (1982).
31. I. I. Berlin, E. K. Kalinin, V. V. Kostyuk, Y. S. Kochelaev, I. V. Pojey and C. A. Jarko, Investigation of natural convection film boiling crisis, *Inzh.-fiz. Zh.* **24,** 205–210 (1973).
32. S. Nishio, Cooldown of insulated metal plates, *Proc. ASME–JSME Thermal Engng Joint Conf.*, Vol. 1, pp. 103–109 (1983).
33. S. Nishio, Study on the minimum heat flux point for boiling heat transfer on a horizontal flat plate (effects of transients and thermal conductance of surface), *Heat Transfer—Jap. Res.* **15,** 15–33 (1986).
34. W. Peyayopanakul and J. W. Westwater, Evaluation of the unsteady-state quenching method for determining boiling curves, *Int. J. Heat Mass Transfer* **21,** 1437–1445 (1978).
35. A. Sakurai, M. Shiotsu and K. Hata, Transient heat transfer after stable film destruction at the minimum film boiling point, *Proc. 21st National Heat Transfer Symp. Japan*, pp. 469–471 (1984).
36. K. J. Baumeister and F. F. Simon, Leidenfrost temperature—its correlation for liquid metals, cryogens, hydrocarbons, and water, *Trans. Am. Soc. Mech. Engrs*, Series C, *J. Heat Transfer* **95,** 166–173 (1973).
37. R. E. Henry, A correlation for the minimum film boiling temperature, *A.I.Ch.E. Symp. Ser.* **70**(138), 81–90 (1974).
38. S. Nishio and M. Hirata, Direct contact phenomena between a liquid droplet and high temperature solid surface, *Proc. 6th Int. Heat Transfer Conf.*, Vol. 1, pp. 245–250 (1978).
39. F. S. Gunnerson and A. W. Cronenberg, On the minimum film boiling conditions for spherical geometries, *Trans. Am. Soc. Mech. Engrs*, Series C, *J. Heat Transfer* **102,** 335–341 (1980).
40. C. J. Scott, Transient experimental techniques for surface heat flux rates. In *Measurements in Heat Transfer* (Edited by E. R. G. Eckert and R. J. Goldstein), pp. 375–396. Hemisphere, Washington (1976).
41. A. Sakurai, M. Shiotsu and K. Hata, Film-boiling heat transfer on horizontal cylinder (II), *Proc. 21st National Heat Transfer Symp. Japan*, pp. 466–468 (1984).
42. L. L. Giventer and J. L. Smith, Jr., Transient pool boiling of liquid nitrogen due to a square-wave heat flux, *Adv. Cryogen. Engng* **15,** 259–270 (1969).
43. H. Merte, Jr. and J. A. Clark, Boiling heat transfer with cryogenic fluids at standard, fractional, and near-zero gravity, *Trans. Am. Soc. Mech. Engrs*, Series C, *J. Heat Transfer* **86,** 351–359 (1964).
44. A. Sakurai, M. Shiotsu and K. Hata, Effect of system pressure on film-boiling heat transfer, minimum heat flux, and minimum temperature, *Nucl. Sci. Engng* **88,** 321–330 (1984).
45. S. Toda and M. Mori, Subcooled film boiling and the behavior of vapor film on a horizontal wire and a sphere, *Proc. 7th Int. Heat Transfer Conf.*, Vol. 4, pp. 173–178 (1982).
46. K. Nishikawa, S. Hasegawa, N. Kitayama and K. Sakamoto, The effects of heating surface conditions on the transition boiling, *Technol. Reports Kyushu Univ.* **38,** 399–404 (1966).
47. F. S. Gunnerson and A. W. Cronenberg, A correlation for the Leidenfrost temperature for spherical particles and its application to FCI analysis, *Trans. Am. Nucl. Soc.* **26,** 381–383 (1977).
48. G. P. Nikolayev, V. V. Bychenkov and V. P. Skripov, Saturated heat transfer to evaporating droplets from a hot wall at different pressures, *Heat Transfer—Sov. Res.* **6,** 128–132 (1974).
49. S.-C. Yao and R. E. Henry, An investigation of the minimum film boiling temperature on horizontal surfaces, *Trans. Am. Soc. Mech. Engrs*, Series C, *J. Heat Transfer* **100,** 260–267 (1978).
50. M. Shoji and H. Nagano, Minimum heat flux of saturated pool boiling on a horizontal heated surface, *Trans. Jap. Soc. Mech. Engrs*, Series B **52,** 2431–2436 (1986).
51. H. Merte, Jr. and E. W. Lewis, Boiling of liquid nitrogen in reduced gravity fields with subcooling, Heat Transfer

Lab., Dept. Mech. Engng, Univ. of Michigan, Michigan (1967).
52. D. Hein, V. Kefer and H. Liebert, Maximum wetting temperature up to critical, NUREG/CP-0060, *Proc. First Int. Workshop on Fund. Aspects of Post-dryout Heat Transfer*, pp. 118–136. U.S. Nucl. Reg. Com., Washington (1984).
53. J. H. Lienhard, Correlation for the limiting liquid superheat, *Chem. Engng Sci.* **31,** 847–849 (1976).
54. V. P. Skripov, *Metastable Liquids*, p. 176. Wiley, New York (1974).
55. K. Nishikawa, S. Hasegawa, H. Honda and S. Sakaguchi, Studies on boiling characteristic curve (1st report, the effects of bulk subcooling and surface conditions on heat transfer), *Trans. Jap. Soc. Mech. Engrs* **34,** 134–141 (1968).
56. K. Nishikawa, S. Hasegawa, T. Iwabuchi and Y. Miyabara, Characteristics of transition boiling on the horizontal plate, *Technol. Reports Kyushu Univ.* **38,** 306–311 (1965).
57. V. A. Grigoriev, V. V. Klimenko and A. G. Shelepen, Pool film boiling from submerged spheres, *Proc. 7th Int. Heat Transfer Conf.*, Vol. 4, pp. 387–392 (1982).
58. V. V. Klimenko, Film boiling on a horizontal plate—new correlation, *Int. J. Heat Mass Transfer* **24,** 69–79 (1981).
59. H. J. Sauer, Jr. and K. M. Ragsdell, Film pool boiling of nitrogen from flat surfaces, *Adv. Cryogen. Engng* **16,** 412–415 (1971).
60. V. V. Klimenko, Investigation of transition and film boiling of cryogenic fluid, Author's Abstract of Candidate Thesis, Moscow (1975).
61. O. Tamaki and N. Wakusaka, Experiments of boiling for liquid nitrogen, *Proc. 7th National Heat Transfer Symp. Japan*, pp. 73–76 (1970).
62. E. R. Hosler and J. W. Westwater, Film boiling on a horizontal plate, *ARS J.* **32,** 553–560 (1962).
63. C. Shih, On the film boiling from small spheres and the use of minimum film boiling temperature in the modeling of vapor explosions, Ph.D. Thesis, Univ. of Wisconsin–Madison, Madison (1978).
64. R. C. Kesselring, P. H. Rosche and S. G. Bankoff, Transition and film boiling from horizontal strips, *A.I.Ch.E. Jl* **13,** 669–675 (1967).
65. V. M. Zhukov, G. M. Kazakov, S. A. Kovalev and Yu. A. Kuzma-kichta, Heat transfer in boiling of liquids on surfaces coated with low thermal conductivity films, *Heat Transfer—Sov. Res.* **7,** 16–26 (1975).
66. G. Hesse, E. M. Sparrow and R. J. Goldstein, Influence of pressure on film boiling heat transfer, *Trans. Am. Soc. Mech. Engrs*, Series C, *J. Heat Transfer* **98,** 166–172 (1976).

TECHNIQUE DE PREDICTION DE LA CONDITION DE POINT A FLUX THERMIQUE MINIMAL (MHF) POUR L'EBULLITION EN RESERVOIR ET SATURATION

Résumé—L'hypothèse de température contrôlée pour la condition de point à flux thermique minimal (MHF), dans laquelle la température du point MHF est considérée comme le facteur pilote indépendant de la configuration de la surface et des dimensions, est étudiée inductivement pour l'ébullition en réservoir d'un liquide saturé. On prouve expérimentalement de telles situations de la condition de point MHF. Une formule pour la température du point MHF est développée pour l'effet de pression. Finalement une technique simple basée sur cette formule est présentée pour estimer les effets de la configuration de surface, des dimensions et de la pression sur le flux thermique minimal.

EINE METHODE ZUR VORHERSAGE DER BEDINGUNGEN AM PUNKT DER MINIMALEN WÄRMESTROMDICHTE (MHF) BEI GESÄTTIGTEM BEHÄLTERSIEDEN

Zusammenfassung—Die Hypothese, daß am Punkt minimaler Wärmestromdichte (MHF) Bedingungen herrschen, bei denen die Temperatur des MHF-Punktes als bestimmende Größe angesehen wird, und die unabhängig von der Oberflächenbeschaffenheit und den Abmessungen sind, wird induktiv für gesättigtes Behältersieden untersucht. Zuerst werden die oben genannten Merkmale der Bedingungen am MHF-Punkt experimentell überprüft. Danach wird eine Korrelation für den Einfluß des Systemdruckes auf die Temperatur am MHF-Punkt entwickelt. Zuletzt wird eine einfache, auf dieser Korrelation beruhende Methode zur Bestimmung der Einflüsse von Oberflächenbeschaffenheit, Abmessungen und Systemdruck auf die minimale Wärmestromdichte vorgestellt.

МЕТОДИКА РАСЧЕТА ТЕМПЕРАТУРЫ, СООТВЕТСТВУЮЩЕЙ МИНИМАЛЬНОМУ ТЕПЛОВОМУ ПОТОКУ ПРИ КИПЕНИИ НАСЫЩЕННОЙ ЖИДКОСТИ В БОЛЬШОМ ОБЪЕМЕ

Аннотация—Проведено исследование гипотезы об условии минимизации теплового потока, согласно которой температура, соответствующая минимальному потоку, считается определяющим фактором и предполагается не зависящей от конфигурации поверхности и ее размеров, что доказано экспериментально. Получено критериальное соотношение для температуры, соответствующей минимальному тепловому потоку, в зависимости от давления. На основе этого соотношения разработана простая методика оценки влияния конфигурации поверхности, размеров и давления на минимальный тепловой поток.